Transport in Porous Media (2019) 129:1–23
https://doi.org/10.1007/s11242-019-01274-2

Modelling of Flow Through Porous Media Over the Complete Flow Regime

Ashes Banerjee[1] · Srinivas Pasupuleti[1] · Mritunjay Kumar Singh[2] · Sekhar Chandra Dutta[1] · G. N. Pradeep Kumar[3]

Received: 5 September 2018 / Accepted: 21 March 2019 / Published online: 1 April 2019

Abstract
A mathematical model is developed based on the empirical power law equation for post-laminar flow through porous media. Hydraulic conductivity and the critical Reynolds number are used as boundary conditions. The developed model can predict hydraulic gradients for specific velocities, irrespective of the media sizes or porosities, over the complete flow transition. Therefore, the model can be very useful to recognise the specific flow regime or to predict the velocity and hydraulic gradient for a given flow regime. A parametric study is carried out concerning the behaviour of binomial (Forchheimer) and power law (Izbash and Wilkins) coefficients subjected to different media sizes, porosities and flow regimes. The observed behaviour of Forchheimer and Izbash coefficients with different media sizes and porosities are similar to the experimental results reported in the literature. However, the values of these coefficients differ when subjected to different flow regimes for any specific packing. The ratios of non-Darcy and Darcy coefficients of the Forchheimer equation suggest an increasing influence of inertia towards the turbulent regime. The maximum and minimum values of β are found to be 1.38 and 0.69 for laminar and turbulent regime, respectively. However, these values are found to be unaffected by the media size and porosity variation. The value of Wilkins coefficient w in the laminar regime is found to be 4841.72 for all media sizes and porosities. However, the coefficient represents a decreasing variation trend towards the turbulent regime which is also dependent of the media size variation.

Keywords Flow modelling · Porous media · Post-laminar flow · Binomial equation · Power law equation

✉ Srinivas Pasupuleti
srinivas@iitism.ac.in

[1] Department of Civil Engineering, Indian Institute of Technology (Indian School of Mines), Dhanbad, Jharkhand 826004, India

[2] Department of Applied Mathematics, Indian Institute of Technology (Indian School of Mines), Dhanbad, Jharkhand 826004, India

[3] Department of Civil Engineering, SVU College of Engineering, Sri Venkateswara University, Tirupati, A.P. 517502, India

1 Introduction

Modelling of velocity and hydraulic gradient relationship through porous media is prerequisite for understanding multiple events such as seepage of ground water and flow through aquifers, flow of oil and gases in the petroleum exploration, flow of water through rock-fill dams, water filters, and fractured rocks, etc. According to the pioneering study of Henry Darcy, the flow velocity is a linear function of head loss through any porous packing. The linear model developed by Darcy has been used explicitly to understand the flow phenomena through porous media over the years. However, the actual head losses are often observed to be higher than the predicted values by Darcy's law; especially when subjected to higher velocities (Trussell and Chang 1999). Such observation may lead to the conclusion that the linear relationship between velocity and the hydraulic gradient is not applicable for all cases, especially for high velocity flows (Hassanizadeh and Gray 1987).

The shift from Darcy's linear model is often credited to the increasing influence of inertia in higher flow rates. Based on the resisting forces, flow through porous media can be divided into three principal flow regimes, i.e. laminar, transition and turbulent (Bear 1972). Shift from laminar to transition and further to turbulent is often represented by Reynolds number which is defined as the ratio of inertia force to the viscous force. The definition and the limiting value of Reynolds number in the literature differ due to the complexities associated with the packing (Dybbs and Edwards 1984; Hellström and Lundström 2006; Horton and Pokrajac 2009; Kovacs 1971; Kundu et al. 2016; Seguin et al. 1998a, b).

Viscous force is the main resistive force in the laminar regime and is generally modelled and described by Darcy's linear equation. However, as the flow velocity/Reynolds number increases, effect of inertial resistance increases (Larsson et al. 2018). Therefore, correction to Darcy's linear equation and use of a non-linear form of equation is apparent to relate hydraulic gradient with velocity in the post-laminar regime (Lasseux and Valdés-Parada 2017). The experimentally obtained velocities and hydraulic gradients from any porous packing represent a binomial or power law-type relation in the post-laminar regime expressed as Eqs. (1) and (2), respectively (Bordier and Zimmer 2000; Chen et al. 2015b; Lacey 2016; Mathias and Todman 2010; Moutsopoulos et al. 2009; Qian et al. 2005; Salahi et al. 2015; Sedghi-Asl et al. 2013, 2014; Wen et al. 2006).

$$-i = av + bv^2 \tag{1}$$

$$-i = mv^j \tag{2}$$

where i is the hydraulic gradient; v (m/s) is the superficial velocity; a (s/m) and b (s^2/m^2) are the Darcy and non-Darcy coefficients, m is an empirical coefficient, and j is an exponent which varies between values 1–2 (Chen et al. 2015a; Sedghi-Asl et al. 2013), respectively. The negative hydraulic gradients in these equations indicate that in a spontaneous process, the flow of fluid must take place from a higher head (total pressure) to a lower head (total pressure). However, since the objective of the present study is to understand the relation between the numerical values of hydraulic gradient and superficial velocity in the post-laminar regime, only the magnitude of these parameters are used in further sections.

The binomial and power law relations presented as Eqs. (1) and (2) are also known as Forchheimer and Izbash equation, respectively. The Forchheimer equation represents the total head loss as a summation of the resistance offered by the viscous effect (av) and the inertial effect (bv^2) in the post-laminar regime. In the laminar regime, the effect of inertial resistance is negligible; therefore, the second order term (bv^2) becomes insignificant, and the Forchheimer equation converts into the form of Darcy's linear equation. Similarly, in

the turbulent regime, the effect of viscous resistance is negligible; therefore, the hydraulic gradient is only a function of the second order term (bv^2) (Chen et al. 2003; Fand et al. 1987; Munson et al. 2006; Skjetne and Auriault 1999).

Extensive experimental studies suggest that the Darcy and non-Darcy coefficients of the Forchheimer equation are functions of large set of field, media and fluid properties such as media size (Huang et al. 2013; van Lopik et al. 2017; Nezhad et al. 2019; Salahi et al. 2015), degree of packing (Banerjee et al. 2018b; Boomsma and Poulikakos 2002; Dan et al. 2016), convergent angle (Banerjee and Pasupuleti 2019; Reddy and Rao 2006; Thiruvengadam and Kumar 1997; Venkataraman and Rao 2000), pore geometry (van Lopik et al. 2017; Macini et al. 2011) Reynolds number (Sidiropoulou et al. 2007) etc. However, the variation trends reported by different researchers lack resemblance and therefore despite numerous reported results, the variation pattern and the behaviour of the Forchheimer coefficients (Darcy and non-Darcy coefficient) remain quite complex and ambiguous till date (Banerjee et al. 2018b; Dukhan et al. 2014; Thiruvengadam and Kumar 1997). Furthermore, some experimental results reported in the literature advocates different values of Darcy and non-Darcy coefficients for the transition and turbulent regimes (Dukhan et al. 2014; Dukhan and Ali 2012; Lage et al. 1997). However, the experiments performed to understand the behaviour of Darcy and non-Darcy coefficients does not adequately acknowledge the effect of flow transition which may be a significant factor concerning the complex behaviour of these coefficients. The transition from laminar to turbulent regime is a gradual process (Dudgeon 1966), and in each phase of transition, the magnitude of viscous and inertial resistance may differ. Therefore, understanding the effect of flow transition over the Darcy and non-Darcy coefficients is a prerequisite for understanding and efficient modelling of these coefficients.

Similar observations can be made for the coefficient m of Izbash equation. Being the only coefficient, m accounts for all the variations in field, media and fluid parameters. Therefore, predicting the value of m for a given set of conditions is quite cumbersome. To reduce such obscurity, Eq. (2) is later modified by Wilkins (1955) after replacing the coefficient m of Izbash equation as a function of pore size of the packing (hydraulic radius) and fluid viscosity as

$$v = C\mu^{\alpha} r^{\beta} i^{\gamma} \tag{3}$$

where μ (Pa s) is the dynamic viscosity of the fluid; r (m) is the hydraulic radius; C, α, β and γ are the coefficients of Wilkins equation. For a given fluid, Eq. (3) can be presented as

$$v = wr^{\beta} i^{\gamma} \quad \text{with } w = C\mu^{\alpha}; \tag{4}$$

The value of γ is widely presented as the illustration of the flow regime which ranges between 0.5 (fully developed turbulent flow) to 1 (laminar flow) (Giroud and Kavazanjian Jr 2014). The limited experimental results available in the literature on Wilkins coefficients point towards a non deviating behaviour of these coefficients with the variation in media size and porosity (Banerjee et al. 2018a, b; Garga et al. 1990; Kumar and Venkataraman 1995; Wilkins 1955). However, resembling the Forchheimer coefficients, the behaviour of Wilkins coefficients are reported for specific flow regimes (value of γ), and the effect of variation in flow regime have never been considered. Therefore, it is not viable to use the results reported in the literature universally without understanding the behaviour of these coefficients over the complete zone of transition from laminar to turbulent.

The present study is therefore initiated to model the velocity and hydraulic gradient relationship over the complete flow transition. The power law-type equation is especially significant for modelling the post-laminar flow because its exponent j represents the gradual

transition of flow from laminar to the turbulent regime. The value of j is 1 when the flow is laminar and gradually increases as the flow shifts towards its maximum value 2 in the turbulent regime. Therefore, given a constant hydraulic gradient, alteration in the flow velocity due to the variation in flow regime can easily be accounted with the power law-type equation. On the other hand, there is no proper representation for flow regimes in the binomial-type equation. The hydraulic gradient in any flow regime depends on the values of Darcy and non-Darcy coefficients which are also functions of various factors associated with the packing as discussed earlier. Therefore, the traditional power law equation/Izbash equation (Eq. 2) is used in the present study to develop the model. Furthermore, the behaviour of the coefficients of the binomial and power law equations are also investigated for different flow regimes. The developed model can predict the velocity corresponding to any hydraulic gradient for the complete flow regime (laminar to turbulent) packed with a given media size and porosity. This in turn may aid the designers and engineers to estimate the velocity and discharge through any hydraulic structure related to porous media flow.

2 Methodology and Model Development

Following assumptions are made prior to the analysis:

- Flow is steady and one dimensional.
- Media is homogeneously packed and porosity of the media is uniform.
- The flow path is assumed to be straight and undeviating through the porous packing.

The power law or Izbash equation (Eq. 2) can be presented as

$$i = mv^j \tag{5}$$

After modification, Eq. (5) can be presented as

$$\log i = \log m + j \log v \tag{6}$$

The mean square error E can be expressed as follows

$$E = \sum_{s=1}^{n} \left[\log i_s - (\log m + j \log v_s)\right]^2 \tag{7}$$

where E is a function of m and j for given values of velocity (v) and hydraulic gradient (i). Therefore, to achieve the minimum value of E, $\frac{\mathrm{d}E}{\mathrm{d}j}$ and $\frac{dE}{dm}$ has to be zero.

From the first condition $\frac{\mathrm{d}E}{\mathrm{d}j} = 0$; it can be concluded that

$$\sum_{s=1}^{n} \log i_s \log v_s = \log m \sum_{s=1}^{n} \log v_s + j \sum_{s=1}^{n} (\log v_s)^2 \quad \left[\text{assuming } n \text{ number of data points}\right] \tag{8}$$

Similarly, the second condition; $\frac{\mathrm{d}E}{\mathrm{d}m} = 0$ yields

$$\sum_{s=1}^{n} \log i_s = n \log m + j \sum_{s=1}^{n} \log v_s \tag{9}$$

The value of j is obtained after performing numerical operation $(\text{Eq. (8)} \times n) - \left(\text{Eq. (9)} \times \sum_{s=1}^{n} \log v_s\right)$ as follows

$$j = \frac{\sum_{s=1}^{n} \log i_s \sum_{s=1}^{n} \log v_s - n \sum_{s=1}^{n} \log i_s \log v_s}{\left(\sum_{s=1}^{n} \log v_s\right)^2 - n \sum_{s=1}^{n} (\log v_s)^2} \tag{10}$$

$$\gamma = \frac{\left(\sum_{s=1}^{n} \log v_s\right)^2 - n \sum_{s=1}^{n} (\log v_s)^2}{\sum_{s=1}^{n} \log i_s \sum_{s=1}^{n} \log v_s - n \sum_{s=1}^{n} \log i_s \log v_s} \quad (\text{since } \gamma = \frac{1}{j}) \tag{11}$$

For $n=2$, from Eq. (11)

$$\gamma = \frac{\left(\sum_{s=1}^{2} \log v_s\right)^2 - 2\left[(\log v_1)^2 + (\log v_2)^2\right]}{(\log i_1 + \log i_2) \sum_{s=1}^{2} \log v_s - 2\left(\log i_1 \log v_1 + \log i_2 \log v_2\right)} \tag{12}$$

Equation (12) can be modified as

$$\begin{aligned} &\gamma \left[\log i_1 \left(\sum_{s=1}^{2} \log v_s - 2 \log v_1\right) + \log i_2 \left(\sum_{s=1}^{2} \log v_s - 2 \log v_2\right)\right] \\ &= \left(\sum_{s=1}^{2} \log v_s\right)^2 - 2\left[(\log v_1)^2 + (\log v_2)^2\right] \end{aligned} \tag{13}$$

given the values of v_1 and v_2, let's assume that

$$\log v_1 = x_1,\ \log v_2 = x_2 \text{ and } \sum_{s=1}^{2} \log v_s = (\log v_1 + \log v_2) = X_2$$

Therefore, after replacing the values of $\log v_1, \log v_2$ and $\sum_{s=1}^{2} \log v_s$ Eq. (13) can be presented as

$$\gamma\left[\log i_1 (X_2 - 2x_1) + \log i_2 (X_2 - 2x_2)\right] = X_2^2 - 2(x_1^2 + x_2^2) \tag{14}$$

Similarly for $n=3$

$$\gamma = \frac{\left(\sum_{s=1}^{3} \log v_s\right)^2 - 3\left[(\log v_1)^2 + (\log v_2)^2 + (\log v_3)^2\right]}{(\log i_1 + \log i_2 + \log i_3) \sum_{s=1}^{3} \log v_s - 3\left(\log i_1 \log v_1 + \log i_2 \log v_2 + \log i_3 \log v_3\right)} \tag{15}$$

Further,

$$\begin{aligned} &\gamma \left[\log i_1 \left(\sum_{s=1}^{3} \log v_s - 3 \log v_1\right) + \log i_2 \left(\sum_{s=1}^{3} \log v_s - 3 \log v_2\right) + \log i_3 \left(\sum_{s=1}^{3} \log v_s - 3 \log v_3\right)\right] \\ &= \left(\sum_{s=1}^{3} \log v_s\right)^2 - 3\left[(\log v_1)^2 + (\log v_2)^2 + (\log v_3)^2\right] \end{aligned} \tag{16}$$

given the values of v_1, v_2 and v_3, let's assume that

$$\log v_1 = x_1, \log v_2 = x_2, \log v_3 = x_3 \text{ and } \sum_{s=1}^{3} \log v_s = (\log v_1 + \log v_2 + \log v_3) = X_3$$

replacing the values of $\log v_1, \log v_2, \log v_3$ and $\sum_{s=1}^{3} \log v_s$ Eq. (16)

$$\gamma\left[\log i_1(X_3 - 3x_1) + \log i_2(X_3 - 3x_2) + \log i_3(X_3 - 3x_3)\right] = [X_3^2 - 3(x_1^2 + x_2^2 + x_3^2)] \tag{17}$$

Finally, for n number of data points, the equation can be represented in its generalised form as

$$\begin{aligned} &\gamma\left[\begin{array}{l} \log i_1\left(\sum_{s=1}^{n} \log v_s - n \log v_1\right) + \log i_2\left(\sum_{s=1}^{n} \log v_s - n \log v_2\right) \\ \quad + \log i_3\left(\sum_{s=1}^{n} \log v_s - n \log v_3\right) + \cdots \\ \quad + \log i_n\left(\sum_{s=1}^{n} \log v_s - n \log v_n\right) \end{array}\right] \\ &= \left(\sum_{s=1}^{n} \log v_s\right)^2 - n\left[(\log v_1)^2 + (\log v_2)^2 + (\log v_3)^2 + \cdots + (\log v_n)^2\right] \end{aligned} \tag{18}$$

for the values of $v_1, v_2, v_3 \cdots v_n$, it may be assumed that

$$\log v_1 = x_1, \log v_2 = x_2, \log v_3 = x_3, \log v_n = x_n \text{ and}$$
$$\sum\nolimits_{s=1}^{n} \log v_s = (\log v_1 + \log v_2 + \cdots + \log v_n) = X_n$$

Therefore Eq. (18) can be presented as

$$\begin{aligned} &\gamma\left[\log i_1(X_n - nx_1) + \log i_2(X_n - nx_2) + \log i_3(X_n - nx_3) + \cdots + \log i_n(X_n - nx_n)\right] \\ &\quad = \left[X_n^2 - n(x_1^2 + x_2^2 + x_3^2 + \cdots + x_n^2)\right] \end{aligned} \tag{19}$$

The system of equations thus obtained always has one extra unknown as compared to the number of equations. For example, for a given set of velocities (v_1 and v_2) and specific flow regime (known value of γ), Eq. (13) has two unknowns (i_1 and i_2). Similarly Eqs. (13) and (14) have three unknowns (i_1, i_2 and i_3) for the velocity set (v_1, v_2 and v_3). Hence, to close the equation system, the initial velocity (v_1) is assumed to be the velocity required for just overcoming the laminar regime. Therefore, it is assumed that the flow is in the transition regime; however, viscous effect still dominates the flow. As a result, the linear relationship between velocity and the hydraulic gradient can still be applicable at this stage. The initial velocity (v_1) required to overcome the laminar regime is calculated using the following equation.

$$v_1 = \frac{Re_{\text{lim}} \times \mu}{\rho \times d} \tag{20}$$

where $Re_{\lim}$, μ, ρ, and d are the limiting Reynolds number, dynamic viscosity of the fluid (N-s/m^2), density of the fluid (kg/m^3) and the diameter of the media (m), respectively. The limiting value of Reynolds number suggested by Bu et al. (2014) for random packing is used in the present model. However, dissimilar values of the Reynolds numbers are reported for transition from the laminar regime in the literature based on the media size, porosity and type of packing (Bu et al. 2014, 2015; Dybbs and Edwards 1984; Jolls and Hanratty 1966; Latifi et al. 1989). Therefore, a single value of the Reynolds number may not be appropriate for all packing.

The initial hydraulic gradient (i_1) corresponding to the obtained initial velocity (v_1) is then calculated after dividing the initial velocity (v_1) by the hydraulic conductivity (K) of the packing. The hydraulic conductivity (K) of a packing can be experimentally determined after performing a constant head or falling head permeability test. However, in the absence of experimental results, the hydraulic conductivity can be calculated using the standard definition as

$$K = k\frac{\mu}{\rho g} \tag{21}$$

where K is the hydraulic conductivity (m/s), k is the intrinsic permeability (m^2) which represents the properties of the packing, μ and ρ are the dynamic viscosity Pa s and density of the fluid (kg/m^3) and g is the acceleration due to gravity (m/s^2).

The values of the intrinsic permeability (k) reported by Venkataraman and Rao (1998) for a wide range of media sizes and porosities are plotted against their corresponding hydraulic radius (Fig. 1). The hydraulic radius of the reported media sizes and porosities are calculated using Eq. (22) (Banerjee et al. 2018b; Thiruvengadam and Kumar 1997)

$$r = \frac{e}{s_0} \tag{22}$$

where, e is the void ratio$=\frac{f}{(1-f)}$ with f is the porosity and s_0 is the specific surface (/m) of the media; calculated as:

$$s_0 = \frac{\alpha}{d} \tag{23}$$

where d is the diameter of the media, and α is known as the shape factor. For spheres the value of α is 6 and for irregular shaped gravels the average value of α is calculated as 8.8 (Thiruvengadam and Kumar 1997). Finally, the relation presented as Eq. (24) is obtained using the best fit method between intrinsic permeability and hydraulic radius from Fig. 1.

$$k = 0.000496\, r^{1.381181} \tag{24}$$

The intrinsic permeability obtained from Eq. (24) can be used to calculate the hydraulic conductivity for a given fluid which is essential for the calculation of the initial hydraulic gradient (i_1) corresponding to the initial velocity (v_1).

After incorporating v_1 and i_1 in Eq. (13), the hydraulic gradient i_2 can be calculated for a given value of v_2. Similarly, the hydraulic gradients ($i_3, i_4 \cdots i_n$) corresponding to a known set of velocities ($v_3, v_4 \cdots v_n$) can be calculated using the developed equation series. A computer programme can be developed using the prepared model for the calculation of hydraulic gradients corresponding to specific velocities for a given media size and porosity. A stepwise methodology is presented in "Appendix" which can aid to develop a programme in any programming language.

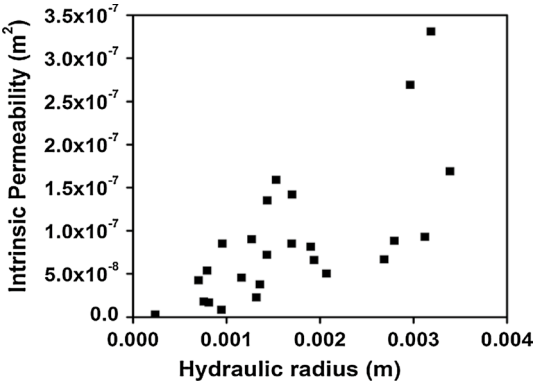

Fig. 1 Variation of intrinsic permeability (k) with hydraulic radius (r), (data of Venkataraman and Rao (1998))

Hydraulic conductivity is the representation of the pore geometry in the developed model, which includes the effect of factors such as interlinking and angularity of the media which are otherwise very difficult to measure. Therefore, with accurate values of hydraulic conductivity, the model can account for such complex parameters. Furthermore, the model can be used for the development of theoretical plots which can be readily utilised to determine the hydraulic gradient for a known velocity through any media size packed with specific porosity. Thus, the model can be convenient for designers and engineers while estimating and predicting discharge through hydraulic structures which are subjected to post-laminar flow such as flow through aquifers, filter beds, rock-fill dams, etc.

3 Model Validation

Values of velocities and corresponding hydraulic gradients obtained from the present model are validated with the experimental results reported by Banerjee et al. (2018b), Cheng et al. (2008) and Sedghi-Asl et al. (2014). The reported media sizes and porosities in the mentioned literature are used to calculate the hydraulic radius. The corresponding intrinsic permeability and hydraulic conductivities are calculated using Eqs. (24) and (21). After calculating the hydraulic conductivities, the velocities corresponding to the reported hydraulic gradients are calculated following the method described in the Methodology and Model development section. The limiting Reynolds number reported by Bu et al. (2015, 2014) for random and structured porous media is used for validating the model. Finally, velocities obtained from the model are plotted with the reported results in the mentioned literature for the same hydraulic gradients. Figure 2a–c represents the comparison of results obtained from the model with the experimental results reported by Banerjee et al. (2018b) for 29.8 mm, 34.78 mm and 41.59 mm crushed stones, respectively. Similar comparisons are presented in Fig. 2d, e with the experimental results reported by Cheng et al. (2008) and Sedghi-Asl et al. (2014). Furthermore, the results from the model are also compared with the unpublished experimental results obtained by the authors from the experimental set-up presented in Banerjee et al. (2018a, b) with glass spheres of 17.51 mm, 25.46 mm and 33.42 mm packed with 47.26%, 51.93% and 54.01% porosity, respectively, in Fig. 2f.

The similarities observed between the reported experimental results and the model outputs advocate the validity of the present model. The deviations whatsoever observed as compared to the experimental results may be attributed to the value of the limiting Reynolds number and the hydraulic conductivity used in the model. Values of both the

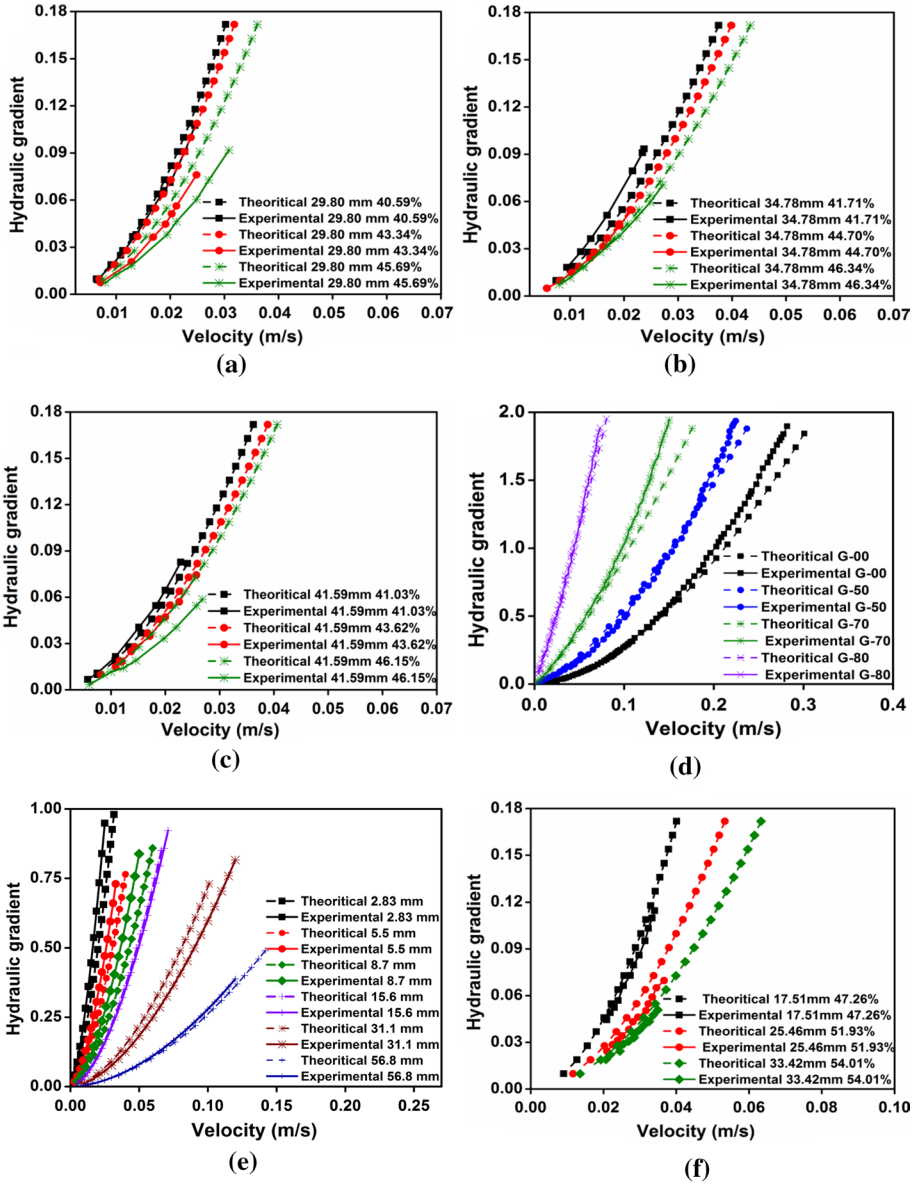

Fig. 2 Comparison of theoretical results with the experimental results for **a** 29.8 mm crushed stones, **b** 34.78 mm crushed stones, **c** 41.59 mm crushed stones reported by Banerjee et al. (2018b), **d** results from Cheng et al. (2008), **e** results obtained by Sedghi-Asl et al. (2014), **f** unpublished data by the authors from glass spheres packed with different porosity

parameters used for validation are determined from the reported literature (Bu et al. 2014, 2015; Venkataraman and Rao 1998). However, due to the complexity associated with the packing, their values vary for different media sizes, porosities as well as with the packing conditions. For that reason, there is no universal relation available to accurately estimate

the hydraulic conductivity and critical Reynolds number for a given packing. Therefore, to achieve results with higher precision, the critical Reynolds number of flow, as well as the hydraulic conductivity used in the model, should be carefully determined for each packing.

4 Results and Discussions

After validating the model outputs with the experimental data reported in the literature, hydraulic gradients corresponding to the different velocities are calculated for 5 mm, 10 mm, 20 mm, 30 mm, 40 mm and 50 mm media sizes each packed with 30%, 35%, 40%, 45%, and 50% porosities. The values of γ (representation of the flow regime) are selected at a regular interval of 0.1 ranging from its minimum value 0.5 (turbulent flow) to the maximum value 1 (laminar flow) to understand the variation of velocity with hydraulic gradient over the complete transition zone (from laminar to turbulent). The velocities and hydraulic gradients corresponding to different flow regimes obtained from 50 mm media diameter are presented in Fig. 3a–f. Similar plots are obtained for other reported media sizes. These plots can be very useful to develop ready to use charts relating the velocities and hydraulic gradients corresponding to different media sizes and porosities for different flow regimes. This type of charts can be of immense help to understand the flow regime for a given velocity and hydraulic gradient from any hydraulic structure or to estimate the hydraulic gradients for a given velocity in different flow regimes.

The velocities and hydraulic gradients calculated from the model are further used to understand the behaviour of binomial and power law-type equations in different flow regimes which are elaborated in later sections.

4.1 Behaviour of the Coefficients of Binomial Equations in Different Flow Regimes

The Darcy and non-Darcy coefficients have been subjected to extensive experimental and theoretical investigation over the years. However, the effect of different flow regimes on Forchheimer coefficients has rarely been addressed in the literature. The present study investigates the behaviour of Darcy and non-Darcy coefficients of the Forchheimer equation with the variation in flow regime through porous media.

The velocities obtained from the different media sizes and porosities are plotted for corresponding hydraulic gradients and different flow regimes similar to Fig. 3. Values of the Darcy and non-Darcy coefficients are calculated after fitting a binomial curve to the data using the best fit method. The Darcy and non-Darcy coefficients are observed to be a function of the velocity range. The experimental outcomes from the literature have reported similar observation (Antohe et al. 1997; Lage et al. 1997; Ovalle-Villamil and Sasanakul 2019). Therefore, it is essential to mention the range of the velocity before analysing the behaviours of these coefficients. In the present study, the Darcy and non-Darcy coefficients are calculated for the velocity range of 0.03 m/s to 0.21 m/s with a standard deviation of 0.01 m/s.

Obtained values of non-Darcy and Darcy coefficients in the different flow regimes are plotted in Figs. 4a–f and 5a–f. The figures represent a decreasing variation trend of the Darcy and non-Darcy coefficients with an increase in media size and porosity. Similar observations are reported in the literature from the experimental outcomes. Furthermore, the behaviour of Darcy and non-Darcy coefficients are investigated for the transition period (laminar to turbulent). The non-Darcy coefficient which is a representation

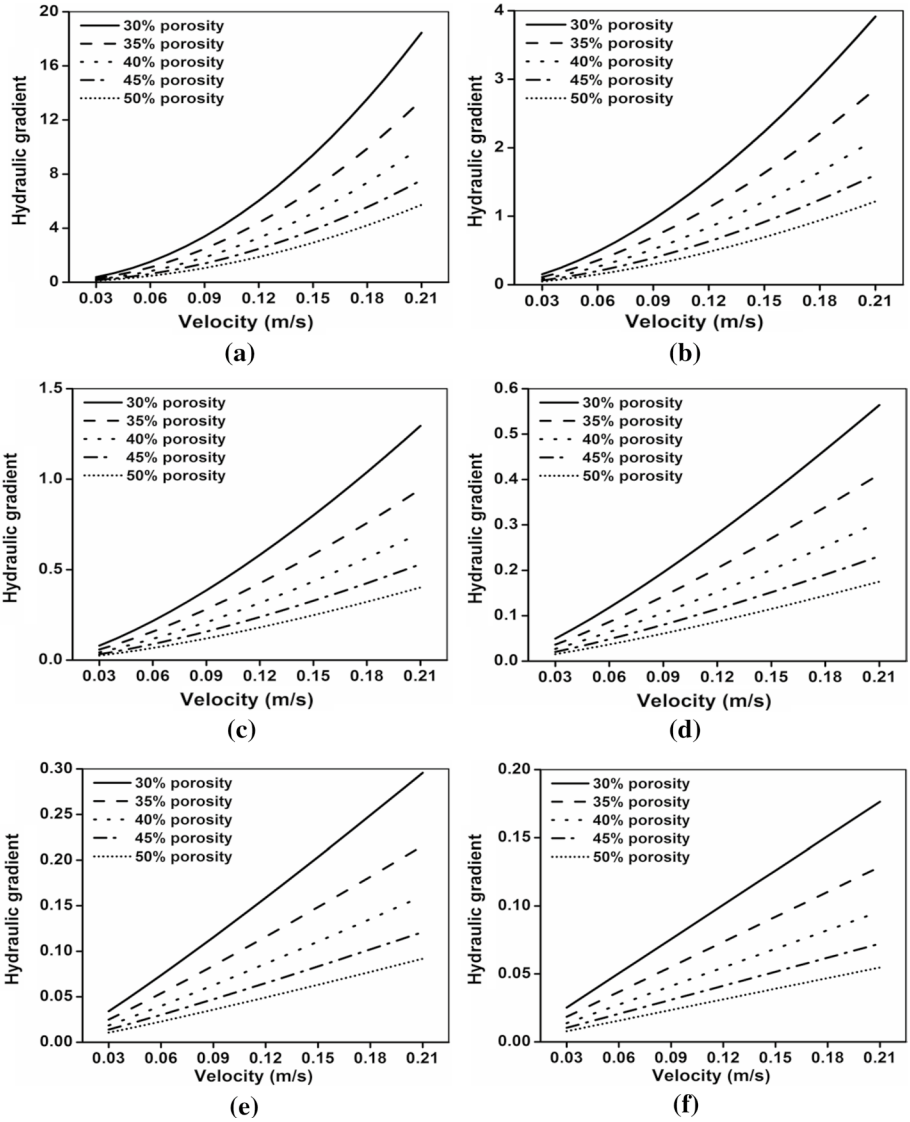

Fig. 3 Variation of velocity with the hydraulic gradients for 50 mm media sizes packed with different porosities at different flow regimes with **a** $\gamma = 0.5$, **b** $\gamma = 0.6$, **c** $\gamma = 0.7$, **d** $\gamma = 0.8$, **e** $\gamma = 0.9$, **f** $\gamma = 1$

of the pressure loss due to the inertia force represents a decreasing trend towards the laminar regime irrespective of media size and porosity of the packing (Fig. 4a–f). However, with the variation in media size and porosity, the Darcy coefficients represent a steady transition in its variation pattern with the flow regime (Fig. 5a–f). In the case of flow through smaller pore sizes, the viscous force between the media boundary and the fluid exerts a significant influence on the total resistance and it increases as the flow shifts towards the laminar regime. This may be the reason for the slight increasing trend observed in 5 mm media (Fig. 5a). As the porosity of the media (Fig. 5b) increases,

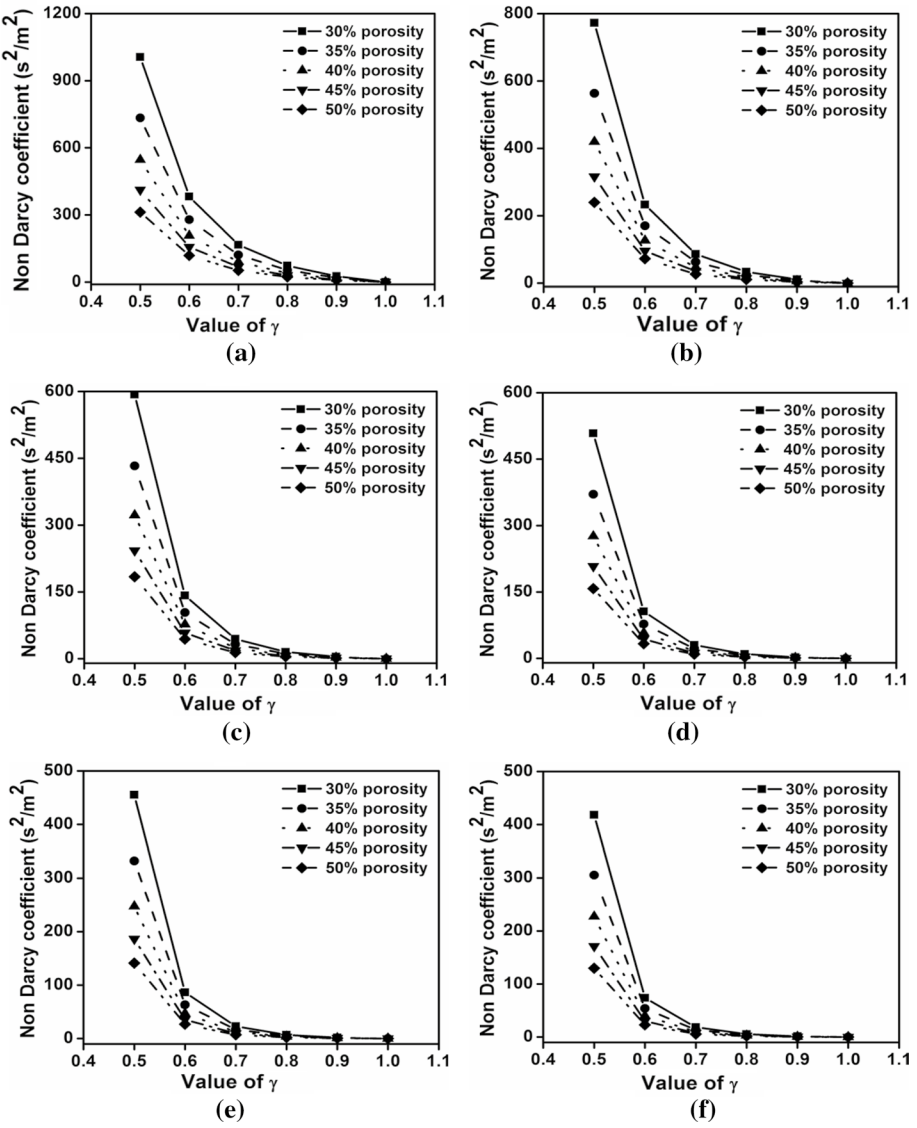

Fig. 4 Variation of non-Darcy coefficient (b) with γ for **a** 5 mm, **b** 10 mm, **c** 20 mm, **d** 30 mm, **e** 40 mm, **f** 50 mm media packed with 30–50% porosity

the value of the Darcy coefficient gradually decreases towards the laminar regime. The increasing influence of the inertia force with the increase in pore size may be the reason for such behaviour. As the pore size of the packing increases, the effect of viscous resistance between the boundary of the packing and the fluid reduces, and the influence of the inertial resistance increases. As a result, for flow through larger pores, the pressure loss is often governed by the inertial resistance. As the flow shifts towards the laminar regime ($\gamma = 1$), the inertial resistance decreases. Since inertia is the dominating

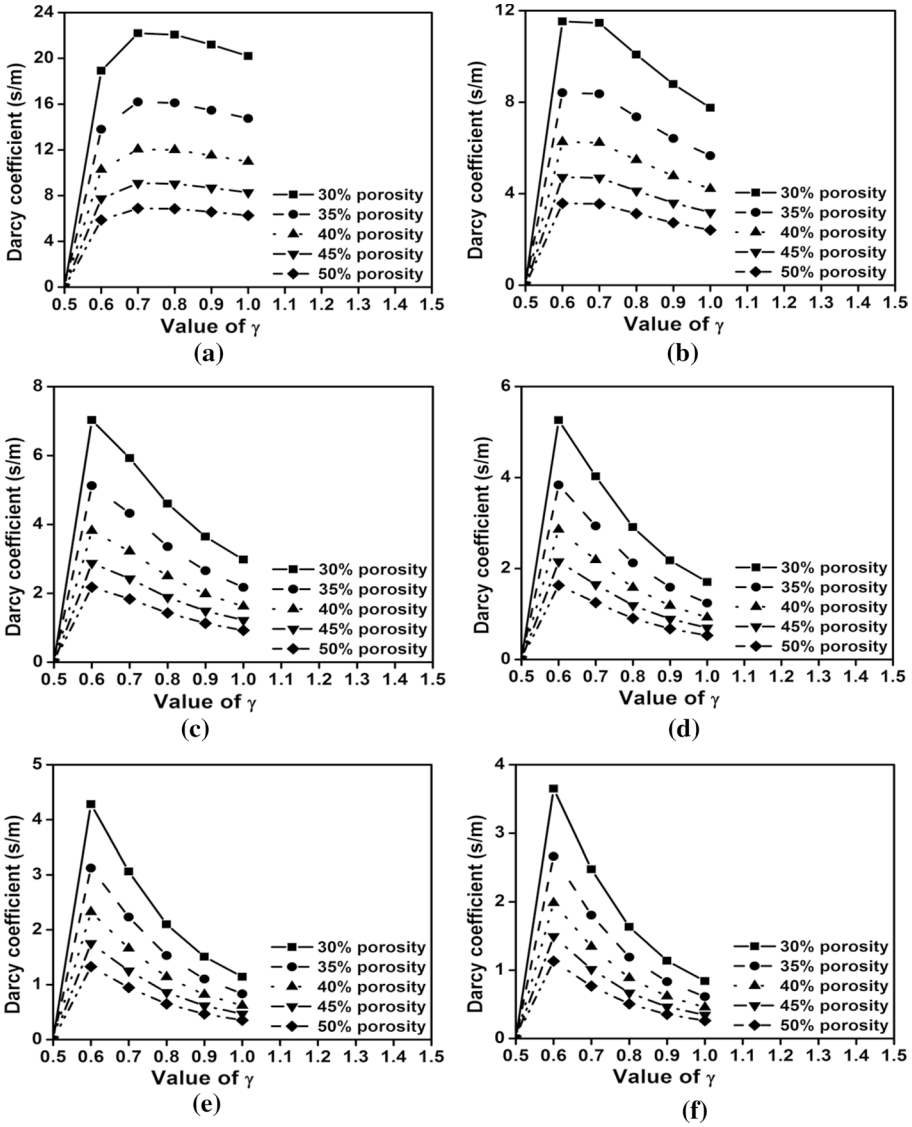

Fig. 5 Variation of Darcy coefficient (a) with γ for **a** 5 mm, **b** 10 mm, **c** 20 mm, **d** 30 mm, **e** 40 mm, **f** 50 mm media packed with 30–50% porosity

force in such conditions, the total head loss also decreases towards the laminar regime. As a result, the Darcy coefficients represent a decreasing variation trend towards the laminar regime for flow through bigger media sizes and higher porosities (Fig. 5c–f). However, when the ratio of the non-Darcy and Darcy coefficients are studied for different flow regimes (γ = .6–0.9), it is evident from Table 1 that the influence of Darcy coefficient or the viscous resistance on the total head loss gradually increases towards the laminar regime. Furthermore, for a given velocity range, the ratios of non-Darcy to

Table 1 Ratio of non-Darcy to Darcy coefficients for different flow regimes when subjected to a constant velocity range

γ	Ratio of non-Darcy to Darcy coefficients					
	5 mm	10 mm	20 mm	30 mm	40 mm	50 mm
0.6	20.22	20.21	20.21	20.19	20.21	20.21
0.7	7.50	7.51	7.50	7.50	7.50	7.51
0.8	3.31	3.31	3.31	3.31	3.31	3.31
0.9	1.23	1.23	1.23	1.23	1.23	1.23
1	0.00	0.00	0.00	0.00	0.00	0.00

Darcy coefficients corresponding to the specific flow regimes are observed to be constant universally.

A similar study is performed to understand the behaviour of Darcy and non-Darcy coefficients for a constant range of hydraulic gradients. The hydraulic gradients are selected between arbitrary ranges of 0.1–0.46 with a standard deviation of 0.02. Velocities corresponding to the mentioned hydraulic gradients are calculated for the given media sizes and porosities. The Darcy and non-Darcy coefficients are calculated from the obtained velocity and hydraulic gradient plots. The coefficients represent similar variation pattern with the flow regime (value of γ). Furthermore, the ratios of non-Darcy to Darcy coefficients for different flow regimes represent an increasing influence of the Darcy coefficient towards the laminar regime (Fig. 6a–f). However, the ratios are not constant for all media sizes and porosities as it is observed for a constant velocity range. The observation confirms that the ratio of viscous and inertial resistance in a specific flow regime primarily depends on the velocity range.

The observation suggests that the variation in media size and porosity has a significant effect on the individual values of the Darcy and non-Darcy coefficients calculated for a given range of velocities or hydraulic gradients. However, the ratios of these coefficients in a specific flow regime are not dependent on pore parameters and are only a function of the velocity range.

Finally, it can be concluded from the analysis that the Forchheimer or binomial equation seems to represent the post-laminar flow through porous media with significant accuracy. However, the coefficients of the equation depend significantly on the flow regime. For a similar media size and porosity, different values of Darcy and non-Darcy coefficients can be observed in different flow regimes. Furthermore, the values of the coefficients are also dependent on the range of the velocity tested in the study. Therefore, specific information on factors such as flow regime, range of velocity and hydraulic gradient is necessary along with different media, fluid and field conditions to accurately predict the values of Darcy and non-Darcy coefficients for flow through porous media.

4.2 Behaviour of Power Law Coefficients in Different Flow Regimes

The coefficient m of the traditional power law equation is reported to have a very obscure variation trend and is very difficult to predict for a given set of media size, porosity or viscosity. On the other hand, the coefficients of Wilkins equations are often reported to be constants in the literature (Banerjee et al. 2018a, b; Garga et al. 1990; Kumar and Venkataraman 1995; Wilkins 1955). However, all the results in the literature are reported for a specific value of γ or j(flow regime). Therefore, behaviour of the coefficients in different flow regimes is still largely unexplored. The developed model provides an insight into the

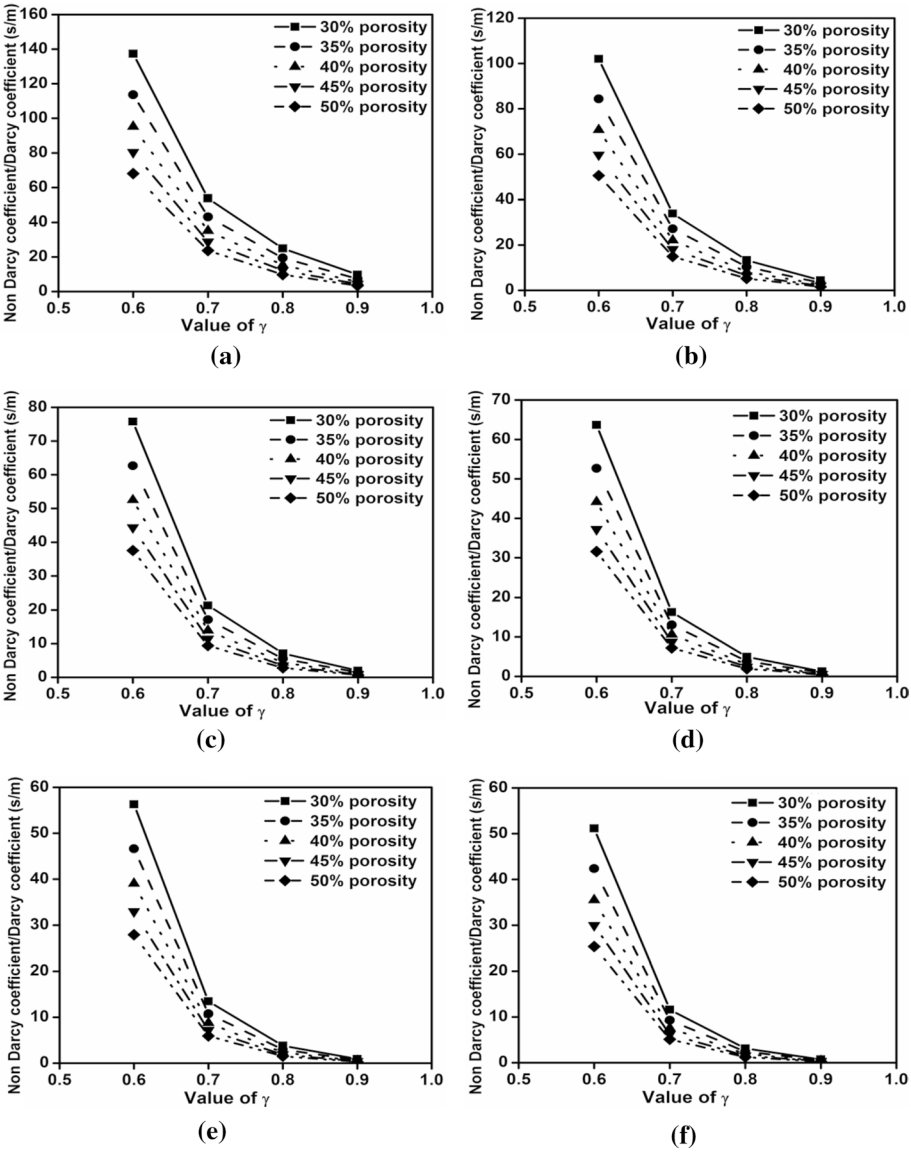

Fig. 6 Variation of the non-Darcy coefficient to Darcy coefficient ratio with γ for **a** 5 mm, **b** 10 mm, **c** 20 mm, **d** 30 mm, **e** 40 mm, **f** 50 mm media packed with 30–50% porosity subjected to a constant hydraulic gradient range

behaviour of the power law and Wilkins coefficients over the complete flow regime (laminar to turbulent).

The coefficients of Izbash equation (m and j) are calculated after fitting power law curve to the obtained velocity and hydraulic gradient plots from the model (Fig. 3). The variation pattern of the coefficient m is plotted with the hydraulic radius for different flow regimes in Fig. 7a–f. The logarithms of the parameters are used in the plot since the actual values

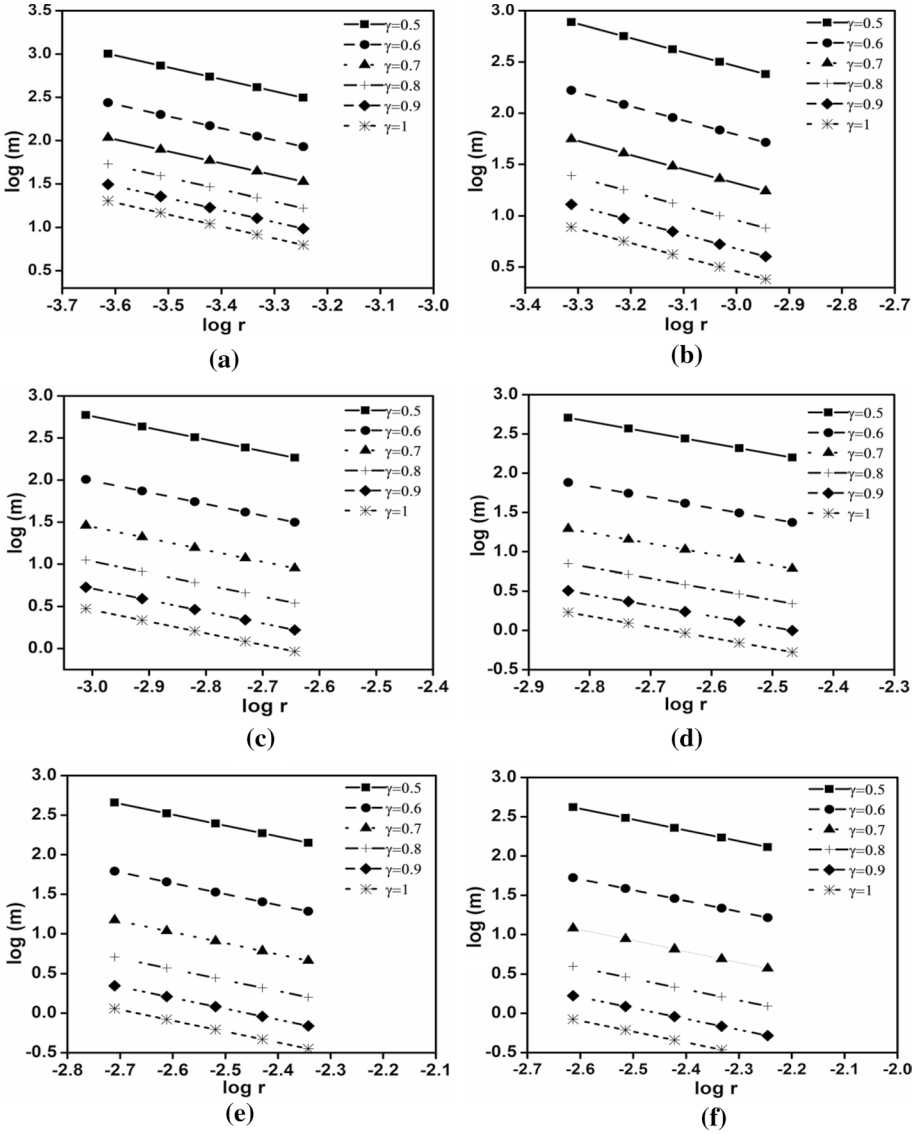

Fig. 7 Variation of Izbash coefficient m with hydraulic radius (r) for **a** 5 mm, **b** 10 mm, **c** 20 mm, **d** 30 mm, **e** 40 mm, **f** 50 mm media

represent a wide range of the variation. An increase in the flow resistance is observed towards the turbulent regime from the plots. Consequently, values of the coefficient m also represent an increasing trend towards the turbulent regime ($\gamma = 0.5$). Furthermore, for a given value of γ, the value of m decreases with an increase in the pore size (hydraulic radius). In view of these observations, the coefficient m can be reported as the representation of the total head loss in any given flow regime. Since m is the only coefficient to account for the variation in total head loss due to different fluid, media and field conditions; predicting the value of m by appropriately accounting for the effects of so many parameters

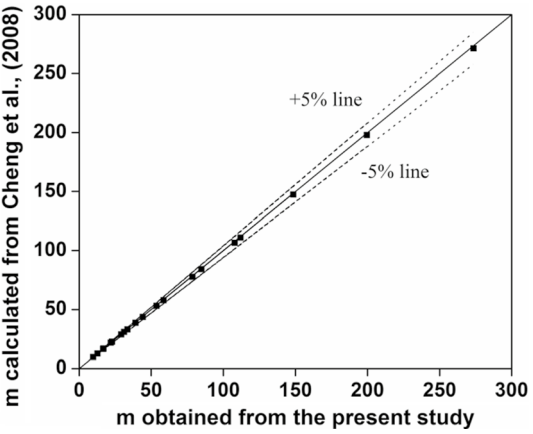

Fig. 8 Comparison of the m value calculated from Cheng et al. (2008) with the m value obtained from the present model

is very difficult. The coefficients of the Izbash equation can be related to the coefficients of the Forchheimer equation with the following formula reported by Cheng et al. (2008)

$$m = \frac{b}{j-1}\left(\frac{a}{b}\frac{j-1}{j-2}\right)^{2-j} \tag{25}$$

The applicability of Eq. (25) is tested in the present study. Obtained values of m from the model are presented with the calculated values of m in Fig. 8. Excellent correlation between the model outputs and the results from Eq. (25) may be observed from Fig. 8.

The coefficients of the Wilkins equation are calculated after obtaining the coefficients of Izbash equation (m and j). As mentioned earlier, the Wilkins equation is a modified form of Izbash equation or the traditional power law equation. Therefore, after comparing Eqs. (2) and (4), following relation can be concluded

$$\left(\frac{1}{m}\right)^{\gamma} = wr^{\beta} \tag{26}$$

Further,

$$\gamma \log\left(\frac{1}{m}\right) = \log w + \beta \log r \tag{27}$$

Finally, the left-hand side of Eq. (27) i.e. $\gamma \log\left(\frac{1}{m}\right)$ is plotted against $\log r$ and a linear equation is fitted to the data (Fig. 9a–f). The slope of the straight line represents the value of coefficient β and the intercept represents the value of $\log w$. Obtained values of the coefficients w and β for different flow regimes are presented in Table 2. The coefficient β represents a constant value for all media sizes and porosities for a given flow regime. However, its values are largely affected by the flow regime (values of γ). The values of coefficient β represent an increasing trend as the flow shifts towards the laminar regime ($\gamma = 1$). Maximum and minimum values of β are found to be 1.38 and 0.69 when the flow is in the laminar and turbulent regime, respectively. Furthermore, values of the coefficient w are observed to be a function of the media size and the flow regime. From Table 2, it can be reported that the coefficient w represents a decreasing trend towards the turbulent regime and with an increase in the media

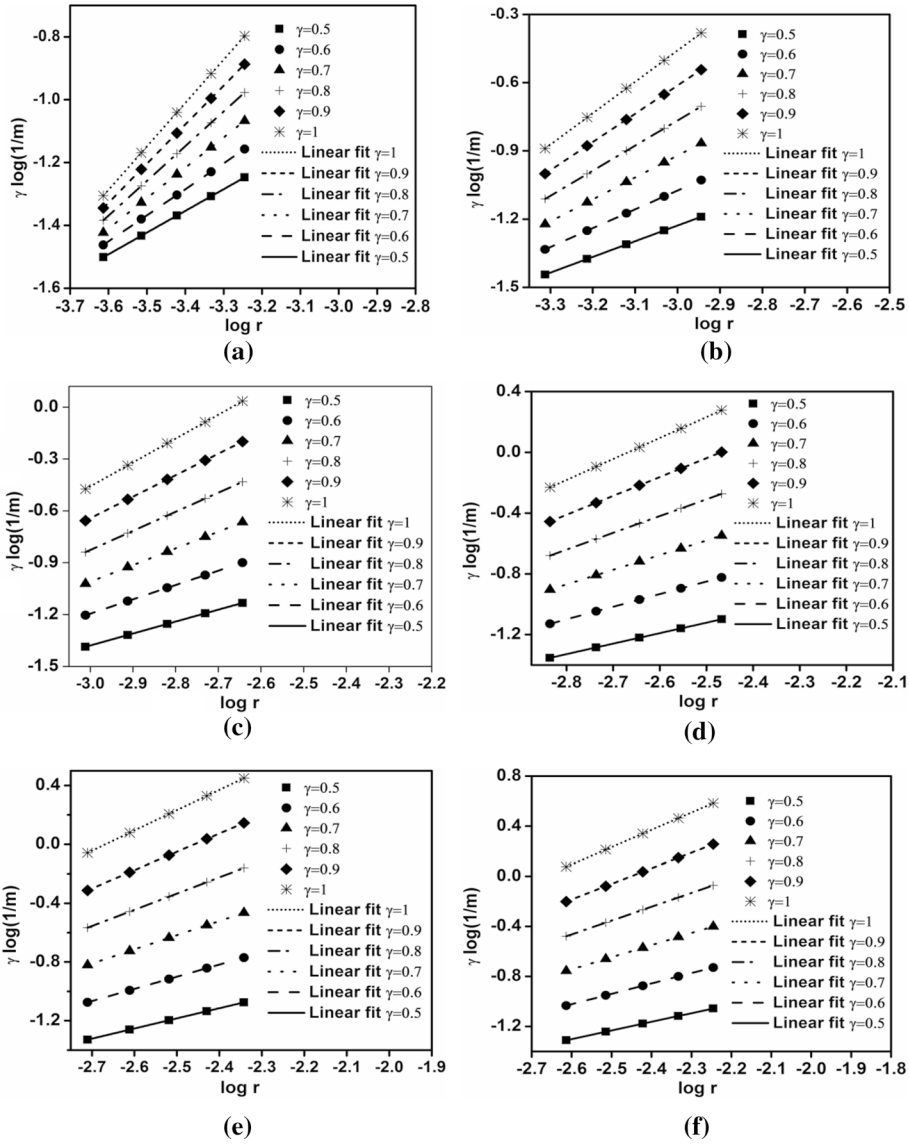

Fig. 9 Variation of $\gamma \log\left({}^{1}/_{m}\right)$ with log(r) for **a** 5 mm, **b** 10 mm, **c** 20 mm, **d** 30 mm, **e** 40 mm, **f** 50 mm media packed with 30–50% porosity in different flow regimes

size. However, at the laminar regime ($\gamma = 1$); numerical values of w and β are observed to be constant (Table 2). Therefore, the coefficient wr^{β} behaves as a parameter only dependent on the media size and porosity; similar to the hydraulic conductivity (K). Therefore it can be concluded that in the laminar regime ($\gamma = 1$) the model outputs are in continuity with Darcy's linear equation validating its applicability in the laminar regime.

Towards the turbulent regime, the effect of media size and porosity becomes predominant over the Wilkins coefficients w. The reason for such behaviour may be attributed to

Table 2 Values of Wilkins coefficients for different media sizes over the complete flow regime

γ	w						β
	Media sizes						
	5 mm	10 mm	20 mm	30 mm	40 mm	50 mm	
0.5	9.86	6.97	4.93	4.03	3.48	3.12	0.69
0.6	34.04	25.76	19.54	16.63	14.83	13.55	0.83
0.7	117.49	95.50	77.62	68.71	62.95	58.88	0.97
0.8	405.51	353.18	307.61	283.79	267.92	255.86	1.10
0.9	1402.81	1309.18	1218.99	1172.20	1137.63	1114.30	1.24
1	4841.72	4841.72	4841.72	4841.72	4841.72	4841.72	1.38

the fact that towards the turbulent regime the inertia effects become more predominant and set up unbalanced forces on account of separation, vortex formation and circulation around the media. The resultant pressure fluctuation and the transverse thrust together with the vortices offers a quite significant resistance to the flow. Towards the turbulent regime, the effect of media size and porosity becomes more predominant on such phenomena and thereby, on the numerical values of coefficient w.

5 Summary and Conclusions

A mathematical model is developed in the present study which can be used to predict velocities corresponding to the specific hydraulic gradients for predefined media sizes and porosities. The obtained velocities from the model are compared and validated with the experimental results reported in the literature. The model can be beneficial to understand the velocity and hydraulic gradient relationship over the complete zone of transition from the laminar regime to the turbulent regime. Behaviour and variation pattern of the coefficients of binomial and power law-type equations with different flow regimes are investigated using theoretically obtained hydraulic gradients and velocities for 5 mm, 10 mm, 20 mm, 30 mm, 40 mm, 50 mm media sizes each packed with 30%, 35%, 40%, 45% and 50% porosities, respectively. The observations from the study may be broadly presented as follows

The coefficient m of the traditional power law-type equation or Izbash equation is a function of media size, porosity as well as the flow regime (γ). Alteration of value in any of the parameters can result in a significant variation in the coefficient m. Therefore, it is very difficult to predict the value of coefficient m for a given set of condition.

Wilkins coefficients β and w are presented as constants in the referred literature for variation in media sizes and porosities. For a given flow regime, the coefficient β is constant for any media size and porosity. However, their values depend primarily on the flow regime (γ). The minimum and maximum value of β corresponding to the turbulent and laminar regime is 0.69 and 1.38. Values of the coefficient w are found to be constants with variation in porosities for a given media size and a specific flow regime. However, its value varies with both media size and flow regime. The influence of the media size variation over the values of coefficient w increases towards the turbulent regime. In the laminar regime, the coefficient w represents constant values for all media sizes and porosities. Therefore, it may

be suggested that the coefficient w is a representation of the irregularities associated with the inertia force in the turbulent regime.

The variation pattern of the Forchheimer coefficients with media sizes and porosities are found to be similar to the results reported in the literature. In a specific flow regime, values of the Darcy and non-Darcy coefficients represent a decreasing trend with an increase in media size and porosity. Furthermore, variation in the flow regime is found to have a significant effect on the coefficients of the binomial equation. The Darcy coefficient is the dominating force near the laminar regime, whereas the influence of the non-Darcy coefficient increases as the flow shifts towards the turbulent regime. However, the values of the Darcy and non-Darcy coefficients are predominantly functions of the total head loss. Since the total head loss increases towards the turbulent regime, values of the Darcy and non-Darcy coefficients also increase. However, the variation pattern of the Darcy coefficient is different for smaller pore sizes (smaller size of media packed with lesser porosity). In the case of flow through smaller media sizes packed with lower porosities, the Darcy coefficient increases as the flow shifts towards the laminar regime. This suggests that for smaller pore sizes viscous resistance is the dominant force and has a significant contribution to the total head loss.

Finally, the study reveals that the shift in flow regime has a significant effect over the velocity and hydraulic gradient relationship in flow through porous media. Irrespective of what type of equation is being used for the modelling, the flow regime should be considered for efficient modelling of post-laminar flow through porous media. Furthermore, the performance of the developed model can be further improved by using specific experimental values of the hydraulic conductivity and critical Reynolds number. With the specific values of the two parameters, the model can be able to predict the flow through porous media universally and therefore may be of considerable help to the engineers and designers to estimate the rate of flow. This, in turn, may also help to design structures associated with post-laminar flow through porous media.

Acknowledgements The authors would like to thank the authorities of IIT (ISM) Dhanbad for their support and in utilising the facilities in various departments. The authors would also acknowledge the funding received from IIT (ISM), Dhanbad under MRP and FRS projects for fabrication of the permeameters, procurement of fluid, media and other accessories utilised for experimentation and investigation.

Compliance with Ethical Standards

Conflict of interest The authors declare that they do not have any conflict of interest.

Appendix

Step Wise methodology to calculate the velocity corresponding to any hydraulic gradient for a certain packing:

Step 1 Input values of critical Reynolds number (Re), media diameter (d), dynamic viscosity (μ), fluid density (ρ)
Step 2 Calculate limiting velocity (v_1) from the relation $v_1 = \frac{Re \times \mu}{\rho \times d}$
Step 3 Insert the hydraulic conductivity (K) of the given packing.

Step 4 Calculate the initial hydraulic gradient (i_1) from the relation $i_1 = \frac{v_1}{K}$
Step 5 Input the value of hydraulic gradient (i_2) for which velocity needs to be measured
Step 6 Specify the required flow regime by incorporating the value of γ. It should be between 0.5 (fully turbulent flow)—1 (laminar flow)
Step 7 Calculate hydraulic gradient (i_2) corresponding to velocity (v_2) from the equation

$$\gamma\left[\log i_1\left(\sum_{s=1}^{2}\log v_s - 2\log v_1\right) + \log i_2\left(\sum_{s=1}^{2}\log v_s - 2\log v_2\right)\right] = \left(\sum_{s=1}^{2}\log v_s\right)^2 - 2\left[(\log v_1)^2 + (\log v_2)^2\right]$$

Step 8 Repeat step 5–7 and calculate hydraulic gradient (i_3) corresponding to velocity (v_3) from the equation stated below:

$$\gamma\left[\log i_1\left(\sum_{s=1}^{3}\log v_s - 3\log v_1\right) + \log i_2\left(\sum_{s=1}^{3}\log v_s - 3\log v_2\right) + \log i_3\left(\sum_{s=1}^{3}\log v_s - 3\log v_3\right)\right] = \left(\sum_{s=1}^{3}\log v_s\right)^2 - 3\left[(\log v_1)^2 + (\log v_2)^2 + (\log v_3)^2\right]$$

Step 9 Similarly calculate hydraulic gradient (i_n) corresponding to velocity (v_n) for from the equation

$$\gamma\left[\begin{array}{l}\log i_1\left(\sum_{s=1}^{n}\log v_s - n\log v_1\right) + \log i_2\left(\sum_{s=1}^{n}\log v_s - n\log v_2\right) \\ \quad + \log i_3\left(\sum_{s=1}^{n}\log v_s - n\log v_3\right) + \cdots \\ \quad + \log i_n\left(\sum_{s=1}^{n}\log v_s - n\log v_n\right)\end{array}\right] = \left(\sum_{s=1}^{n}\log v_s\right)^2 - n\left[(\log v_1)^2 + (\log v_2)^2 + (\log v_3)^2 + \cdots + (\log v_n)^2\right]$$

Step 10 Plot calculated velocities and hydraulic gradients to get the variation trend of velocity with hydraulic gradient in a specific flow regime for a given media size porosity.

References

Antohe, B., Lage, J., Price, D., Weber, R.: Experimental determination of permeability and inertia coefficients of mechanically compressed aluminum porous matrices. J. Fluids Eng. **119**, 404–412 (1997)

Banerjee, A., Pasupuleti, S.: Effect of convergent boundaries on post laminar flow through porous media. Powder Technol. **342**, 288–300 (2019)
Banerjee, A., Pasupuleti, S., Singh, M.K., Kumar, G.: An investigation of parallel post-laminar flow through coarse granular porous media with the Wilkins equation. Energies **11**, 320 (2018a)
Banerjee, A., Pasupuleti, S., Singh, M.K., Kumar, G.N.P.: A study on the Wilkins and Forchheimer equations used in coarse granular media flow. Acta Geophys. **66**, 81–91 (2018b)
Bear, J.: Dynamics of Fluids in Porous Media. Elsevier, New York (1972)
Boomsma, K., Poulikakos, D.: The effects of compression and pore size variations on the liquid flow characteristics in metal foams. J. Fluids Eng. **124**, 263–272 (2002)
Bordier, C., Zimmer, D.: Drainage equations and non-Darcian modelling in coarse porous media or geosynthetic materials. J. Hydrol. **228**, 174–187 (2000)
Bu, S., Yang, J., Dong, Q., Wang, Q.: Experimental study of transition flow in packed beds of spheres with different particle sizes based on electrochemical microelectrodes measurement. Appl. Therm. Eng. **73**, 1525–1532 (2014)
Bu, S., Yang, J., Dong, Q., Wang, Q.: Experimental study of flow transitions in structured packed beds of spheres with electrochemical technique. Exp. Therm. Fluid Sci. **60**, 106–114 (2015)
Chen, C., Wan, J., Zhan, H.: Theoretical and experimental studies of coupled seepage-pipe flow to a horizontal well. J. Hydrol. **281**, 159–171 (2003)
Chen, Y.-F., Liu, M.-M., Hu, S.-H., Zhou, C.-B.: Non-Darcy's law-based analytical models for data interpretation of high-pressure packer tests in fractured rocks. Eng. Geol. **199**, 91–106 (2015a)
Chen, Y.-F., Zhou, J.-Q., Hu, S.-H., Hu, R., Zhou, C.-B.: Evaluation of Forchheimer equation coefficients for non-Darcy flow in deformable rough-walled fractures. J. Hydrol. **529**, 993–1006 (2015b)
Cheng, N.-S., Hao, Z., Tan, S.K.: Comparison of quadratic and power law for nonlinear flow through porous media. Exp. Therm. Fluid Sci. **32**, 1538–1547 (2008)
Dan, H.C., He, L.H., Xu, B.: Experimental investigation on non-Darcian flow in unbound graded aggregate material of highway pavement. Transp. Porous Med. **112**, 189–206 (2016)
Dudgeon, C.R.: An experimental study of the flow of water through coarse granular media. La Houille Blanche. **7**, 785–801 (1966)
Dukhan, N., Ali, M.: Strong wall and transverse size effects on pressure drop of flow through open-cell metal foam. Int. J. Therm. Sci. **57**, 85–91 (2012)
Dukhan, N., Bağcı, Ö., Özdemir, M.: Experimental flow in various porous media and reconciliation of Forchheimer and Ergun relations. Exp. Therm. Fluid Sci. **57**, 425–433 (2014)
Dybbs, A., Edwards, R.: A new look at porous media luid mechanics—Darcy to turbulent. In: Fundamentals of transport phenomena in porous media, vol. 82, pp. 199–256. Springer, Dordrecht (1984)
Fand, R., Kim, B., Lam, A., Phan, R.: Resistance to the flow of fluids through simple and complex porous media whose matrices are composed of randomly packed spheres. J. Fluids Eng. **109**, 268–274 (1987)
Garga, V.K., Hansen, D., Townsend, R.D.: Considerations on the design of flow through rockfill drains. In: 14th Annual British Columbia Mine Reclamation Symposium, Cranbrook, BC (1990)
Giroud, J.P., Kavazanjian Jr., E.: Degree of turbulence of flow in geosynthetic and granular drains. J. Geotech. Geoenvironmental Eng. **140**, 06014001 (2014)
Hassanizadeh, S.M., Gray, W.G.: High velocity flow in porous media. Transp. Porous Med. **2**, 521–531 (1987)
Hellström, G., Lundström, S.: Flow through porous media at moderate Reynolds number. In: Proceedings, 4th International Scientific Colloquium Modelling for Material Processing, pp. 129–134 (2006)
Horton, N., Pokrajac, D.: Onset of turbulence in a regular porous medium: an experimental study. Phys. Fluids **21**, 045104 (2009)
Huang, K., Wan, J., Chen, C., He, L., Mei, W., Zhang, M.: Experimental investigation on water flow in cubic arrays of spheres. J. Hydrol. **492**, 61–68 (2013)
Jolls, K., Hanratty, T.: Transition to turbulence for flow through a dumped bed of spheres. Chem. Eng. Sci. **21**, 1185–1190 (1966)
Kovacs, G.: Seepage through saturated and unsaturated layers. Hydrol. Sci. J. **16**, 27–40 (1971)
Kumar, G.N.P., Venkataraman, P.: Non-Darcy converging flow through coarse granular media. J. Inst. Eng. India Civ. Eng. Div. **76**, 6–11 (1995)
Kundu, P., Kumar, V., Mishra, I.M.: Experimental and numerical investigation of fluid flow hydrodynamics in porous media: characterization of pre-Darcy, Darcy and non-Darcy flow regimes. Powder Technol. **303**, 278–291 (2016)
Lacey, R.: The characteristic flow equation: a tool for engineers and scientists. Geotext. Geomembr. **44**, 534–548 (2016)
Lage, J., Antohe, B., Nield, D.: Two types of nonlinear pressure-drop versus flow-rate relation observed for saturated porous media. J. Fluids Eng. **119**, 700–706 (1997)

Larsson, I.A.S., Lundström, T.S., Lycksam, H.: Tomographic PIV of flow through ordered thin porous media. Exp. Fluids **59**, 96 (2018)
Lasseux, D., Valdés-Parada, F.J.: On the developments of Darcy's law to include inertial and slip effects. Comptes Rendus Mécanique **345**, 660–669 (2017)
Latifi, M., Midoux, N., Storck, A., Gence, J.: The use of micro-electrodes in the study of the flow regimes in a packed bed reactor with single phase liquid flow. Chem. Eng. Sci. **44**, 2501–2508 (1989)
Macini, P., Mesini, E., Viola, R.: Laboratory measurements of non-Darcy flow coefficients in natural and artificial unconsolidated porous media. J. Pet. Sci. Eng. **77**, 365–374 (2011)
Mathias S.A., Todman, L.C.: Step-drawdown tests and the Forchheimer equation. Water Resour. Res. **46**, W07514 (2010)
Moutsopoulos, K.N., Papaspyros, I.N., Tsihrintzis, V.A.: Experimental investigation of inertial flow processes in porous media. J. Hydrol. **374**, 242–254 (2009)
Munson, B.R., Young, D.F., Okiishi, T.H., Huebsch, W.W.: Fundamentals of Fluid Mechanics, p. 69. Wiley, Hoboken (2006)
Nezhad, M.M., Rezania, M., Baioni, E.: Transport in porous media with nonlinear flow condition. Transp. Porous Med. **126**, 5–22 (2019)
Ovalle-Villamil, W., Sasanakul, I.: Investigation of non-Darcy low for fine grained materials. Geotech. Geol. Eng. **37**, 413–429 (2019)
Qian, J., Zhan, H., Zhao, W., Sun, F.: Experimental study of turbulent unconfined groundwater flow in a single fracture. J. Hydrol. **311**, 134–142 (2005)
Reddy, N.B., Rao, P.R.: Effect of convergence on nonlinear flow in porous media. J. Hydraul. Eng. **132**, 420–427 (2006)
Salahi, M.-B., Sedghi-Asl, M., Parvizi, M.: Nonlinear flow through a packed-column experiment. J. Hydrol. Eng. **20**, 04015003 (2015)
Sedghi-Asl, M., Rahimi, H., Farhoudi, J., Hoorfar, A., Hartmann, S.: One-dimensional fully developed turbulent flow through coarse porous medium. J. Hydrol. Eng. **19**, 1491–1496 (2013)
Sedghi-Asl, M., Rahimi, H., Salehi, R.: Non-Darcy flow of water through a packed column test. Transp. Porous Med. **101**, 215–227 (2014)
Seguin, D., Montillet, A., Comiti, J.: Experimental characterisation of flow regimes in various porous media—I: limit of laminar flow regime. Chem. Eng. Sci. **53**, 3751–3761 (1998a)
Seguin, D., Montillet, A., Comiti, J., Huet, F.: Experimental characterization of flow regimes in various porous media—II: transition to turbulent regime. Chem. Eng. Sci. **53**, 3897–3909 (1998b)
Sidiropoulou, M.G., Moutsopoulos, K.N., Tsihrintzis, V.A.: Determination of Forchheimer equation coefficients *a* and *b*. Hydrol. Process. **21**, 534–554 (2007)
Skjetne, E., Auriault, J.-L.: High-velocity laminar and turbulent flow in porous media. Transp. Porous Med. **36**, 131–147 (1999)
Thiruvengadam, M., Kumar, G.N.P.: Validity of Forchheimer equation in radial flow through coarse granular media. J. Eng. Mech. **123**, 696–704 (1997)
Trussell, R.R., Chang, M.: Review of flow through porous media as applied to head loss in water filters. J. Environ. Eng. **125**, 998–1006 (1999)
van Lopik, J.H., Snoeijers, R., van Dooren, T.C., Raoof, A., Schotting, R.J.: The effect of grain size distribution on nonlinear flow behavior in sandy porous media. Transp. Porous Med. **120**, 37–66 (2017)
Venkataraman, P., Rao, P.R.M.: Darcian, transitional, and turbulent flow through porous media. J. Hydraul. Eng. **124**, 840–846 (1998)
Venkataraman, P., Rao, P.R.M.: Validation of Forchheimer's law for flow through porous media with converging boundaries. J. Hydraul. Eng. **126**, 63–71 (2000)
Wen, Z., Huang, G., Zhan, H.: Non-Darcian flow in a single confined vertical fracture toward a well. J. Hydrol. **330**, 698–708 (2006)
Wilkins, J.K.: Flow of water through rockfill and its application to the design of dams. N. Z. Eng. **10**, 382–387 (1955)